Designing Protein Dimerizers: The Importance of Ligand Conformational Equilibria

Jonathan C. T. Carlson,[†] Aaron Kanter,[†] Guruvasuthevan R. Thuduppathy,[†]
Vivian Cody,[§] Pamela E. Pineda,[†] R. Scott McIvor,[‡] and Carston R. Wagner*,[†]

*Department of Medicinal Chemistry, College of Pharmacy, and Department of Cell Biology,
Genetics and Development, University of Minnesota, Minneapolis, Minnesota 55455, and
Hauptman-Woodward Medical Research Institute Inc., 73 High St., Buffalo, New York 14203*

Received March 21, 2002; E-mail: wagne003@tc.umn.edu

Abstract: In an effort to elucidate the role of ligand conformation in induced protein dimerization, we synthesized a flexible methotrexate (MTX) dimer, demonstrated its ability to selectively dimerize *Escherichia coli* dihydrofolate reductase (DHFR), and evaluated the factors regulating its ability to induce cooperative dimerization. Despite known entropic barriers, bis-MTX proved to possess substantial conformational stability in aqueous solution (-3.8 kcal/mol $\geq \Delta G_{fold} \geq -4.9$ kcal/mol), exerting a dominant influence on the thermodynamics of dimerization. To dimerize DHFR, bis-MTX must shift from a folded to an extended conformation. From this conclusion, the strength of favorable protein−protein interactions in bis-MTX−*E. coli* DHFR dimers (-3.1 kcal/mol $\geq \Delta G_c \geq -4.2$ kcal/mol), and the selectivity of dimerization for *E. coli* DHFR relative to mouse DHFR ($>10^7$) could be determined. The crystal structure of bis-MTX in complex with *E. coli* DHFR confirms the feasibility of a close-packed dimerization interface and suggests a possible solution conformation for the induced protein dimers. Consequently, the secondary structure of this minimal foldamer regulates its ability to dimerize dihydrofolate reductase in solution, providing insight into the complex energy landscape of induced dimerization.

Introduction

Biological inducers (or modulators) of protein dimerization, such as erythropoeitin (EPO) and human growth hormone, regulate signal transduction, transcription, and metabolic processes.[1] Mirroring these functions, chemical inducers of protein dimerization (CIDs) have been used to control gene expression,[2,3] modulate cell membrane receptor signaling,[4] selectively antagonize cellular processes,[5−7] search for novel biocatalysts,[8,9] and even to target protein heterodimers with no established ligand.[10] Moreover, CID-based systems may be clinically valuable as a tool to selectively regulate gene expression in cell-based therapies.[11] Despite these diverse applications, regulatory mechanisms governing chemically induced dimerization have been incompletely investigated. Parallels have been drawn to the diverse forms of conformational control that are a hallmark of biological regulation, essential in macromolecular recognition and signal transduction. Receptor conformation, for instance, has recently proven to be crucial in regulating activation of the dimerized EPO receptor,[12,13] and the behavior of synthetic ligands within this model analyzed.[14] Although the role of receptor conformation in these processes is now appreciated, the potentially significant influence of ligand conformation—in both biological and chemical cases—has been largely neglected.

Dimerization exhibits a sensitive interplay between conformational and binding energetics, as increasing ligand concentrations compete for binding to dimerized proteins and ultimately favor monomerization.[15,16] It can be shown, first, that the association constant for binding of ligand to monomeric receptor, K_1, determines the ligand concentration ($K_d = 1/K_1$) at which peak dimerization is observed. Second, the association constant

* Corresponding author address: Department of Medicinal Chemistry, University of Minnesota, 8-174 Weaver Densford Hall, 308 Harvard St. SE, Minneapolis, MN 55455. Phone: 612 625−2614.
 † Department of Medicinal Chemistry, College of Pharmacy.
 ‡ Department of Cell Biology, Genetics and Development.
 § Hauptman-Woodward Medical Research Institute Inc.

(1) Klemm, J. D.; Schreiber, S. L.; Crabtree, G. R. *Annu. Rev. Immunol.* **1998**, *16*, 569−592.
(2) Diver, S. T.; Schreiber, S. L. *J. Am. Chem. Soc.* **1997**, *119*, 5106−5109.
(3) Amara, J. F.; Clackson, T.; Rivera, V. M.; Guo, T.; Keenan, T.; Natesan, S.; Pollock, R.; Yang, W.; Courage, N. L.; Holt, D. A.; Gilman, M. *Proc. Natl. Acad. Sci. U.S.A.* **1997**, *94*, 10618−10623.
(4) Spencer, D. M.; Wandless, T. J.; Schreiber, S. L.; Crabtree, G. R. *Science* **1993**, *262*, 1019−1024.
(5) Briesewitz, R.; Ray, G. T.; Wandless, T. J.; Crabtree, G. R. *Proc. Natl. Acad. Sci. U.S.A.* **1999**, *96*, 1953−1958.
(6) Lin, Y.-M.; Braun, P. D.; Ray, G. T.; Wandless, T. J. In *Abstracts of Papers*, 221st National Meeting of the American Chemical Society, San Diego, CA, 2001; American Chemical Society: Washington, DC, 2001.
(7) Barglow, K. T.; Lin, Y.-M.; Braun, P. D.; Wandless, T. J. *Abstracts of Papers*, 223rd National Meeting of the American Chemical Society, Orlando, FL, 2002; American Chemical Society: Washington, DC, 2002.
(8) Lin, H.; Abida, W. M.; Sauer, R. T.; Cornish, V. W. *J. Am. Chem. Soc.* **2000**, *122*, 4247−4248.
(9) Firestine, S. M.; Salinas, F.; Nixon, A. E.; Baker, S. J.; Benkovic, S. J. *Nature Biotech.* **2000**, *18*, 544−547.

(10) Koide, K.; Finkelstein, J. M.; Ball, Z.; Verdine, G. L. *J. Am. Chem. Soc.* **2001**, *123*, 398−408.
(11) Neff, T.; Blau, C. A. *Blood* **2001**, *97*, 2535−2540.
(12) Livnah, O.; Stura, E. A.; Middleton, S. A.; Johnson, D. L.; Jolliffe, L. K.; Wilson, I. A. *Science* **1999**, *283*, 987−990.
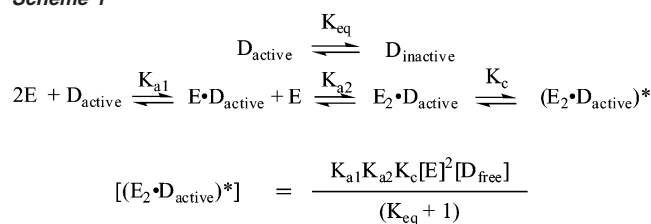(13) Remy, I.; Wilson, I. A.; Michnick, S. W. *Science* **1999**, *283*, 990−993.
(14) Boger, D. L.; Goldberg, J. *Bioorg. Med. Chem.* **2001**, *9*, 557−562.
(15) Perelson, A. S.; DeLisi, C. *Math. Biosci.* **1980**, *48*, 71−110.
(16) Whitty, A.; Borysenko, C. W. *Chem. Biol.* **1999**, *6*, R107−R118.

Scheme 1

$$D_{active} \underset{}{\overset{K_{eq}}{\rightleftharpoons}} D_{inactive}$$

$$2E + D_{active} \underset{}{\overset{K_{a1}}{\rightleftharpoons}} E{\cdot}D_{active} + E \underset{}{\overset{K_{a2}}{\rightleftharpoons}} E_2{\cdot}D_{active} \underset{}{\overset{K_c}{\rightleftharpoons}} (E_2{\cdot}D_{active})*$$

$$[(E_2{\cdot}D_{active})*] = \frac{K_{a1}K_{a2}K_c[E]^2[D_{free}]}{(K_{eq} + 1)}$$

for formation of the ternary complex, K_2, governs the magnitude of the peak response and the width of the dimerization plateau. A significant shortcoming of the current model is that it does not provide a framework for analyzing the individual molecular processes that influence K_1 and K_2. On the basis of these considerations, we proposed an expanded binding model (Scheme 1) which explicitly accounted for the effects of ligand conformational equilibria (K_{eq})[17] and cooperative receptor interactions (K_c) (eq 1). For simplicity of representation, we treat the connection energy—any free energy components, particularly entropic, specific to the bivalent complex—as a component of K_c.[18]

$$[(E_2{\cdot}D_{active})*] = \frac{K_{a1}K_{a2}K_c[E]^2[D_{free}]}{(K_{eq} + 1)} \qquad (1)$$

Clearly, the concentration of functionally active complex $[(E_2{\cdot}D_{active})*]$ depends heavily on both ligand conformation (K_{eq}) and receptor interactions (K_c), which modulate the values of K_{a1} and K_{a2}, respectively. Stated directly, increases in K_{eq} shift peak dimerization to higher ligand concentrations, while increases in K_c broaden and elevate the dimerization plateau.

We surveyed the literature for suitable biological data and found several cases for which the explicit treatment of ligand conformation may be justified. The best evidence appears in the case of EPO and its receptor (for which ligand binding reorganizes the predimerized receptor[12,13]); the NMR-determined solution structure of the hormone[19] differs considerably from the crystallographically observed receptor bound form.[20] Human growth hormone, which acts as a classical dimerizing ligand,[21] also appears to shift conformation on receptor binding, based on a comparison between free[22] and bound[23] crystal structures. The manner in which these conformational changes affect the thermodynamics and kinetics of signaling remains unknown.

Because direct thermodynamic and structural analysis of these effects is rendered difficult by the size and complexity of the cytokine−receptor complexes, we have developed a model system in which the parameters governing dimerization are directly ascertainable. The stringent requirements are several: foremost is the ability to generate efficient dimerization only

in the presence of the ligand. Second, the ligand must bind its receptors with high affinity, to accurately mimic endogenous systems and to allow reproducible experimental observation of the active complex. Third, the conformational behavior of the ligand should be directly observable.

We noted that a binary complex of *E. coli* DHFR (ecDHFR) and methotrexate, although monomeric in solution, crystallized in a dimeric form (PDB accession code: 4DFR).[24] The C_2-symmetric protein dimer is suitably oriented for potential chemical cross-linking: the γ-carboxylate tail of MTX is directly pointed toward its cognate and is sterically uncrowded. Molecular modeling indicated that a 9 to 12 carbon linker should be sufficient to bridge the 9 Å gap between the carboxylates without significantly perturbing the ligand orientation. Moreover, γ-carboxylate derivatization of MTX does not appreciably affect binding.[25] We hypothesized that this synthetic ligand−receptor system would meet the criteria outlined above: the recombinant manipulation of ecDHFR has been extensively exploited and MTX is a tight-binding inhibitor of ecDHFR (sub-nanomolar affinity). Furthermore, the conformational behavior of MTX can be evaluated by NMR.[26] Our design process sought a linker of maximal flexibility, to permit the widest range of suitable bound conformations. The work of Whitesides and co-workers, in an analysis of torsional entropy, implied that methylene-based linkers were more flexible than the analogous ethylene glycols.[27] On the basis of these observations, we synthesized a dimeric ligand (Scheme 2) in which two MTX moieties were bridged by amide bonds to a flexible dodecanediamine linker, MTX₂-C₁₂ (bis-MTX, **5**), and went on to characterize the conformational state and ability of the ligand to induce bacterial and murine DHFR dimerization.

In support of this rationale, Kopytek et al. have recently demonstrated that a dimer of MTX containing a 4,9-dioxa-1,12-dodecanediamine linker (i.e., 10 methylenes and 2 oxygens) was able to partially dimerize ecDHFR.[28]

Results and Discussion

Bis-MTX was synthesized by a core-expansion strategy, beginning with the linker and appending the successive glutamate, PABA, and pteridine moieties segmentally (Scheme 2).

The 1,12-diaminododecane linker was coupled to 2 equiv of Cbz-L-glumatic acid α-methyl ester, in a reaction promoted by EDCI and DMAP, yielding **1**. The Cbz protecting groups of the linker were removed by hydrogenation in the presence of 2 equiv of HCl to produce the hydrochloric amine salt, minimizing diketopiperazine-forming side reactions. Compound **3** was prepared via DCC-mediated coupling with 4-[*N*-methyl-*N*-(trifluoroacetyl)amino]benzoic acid (**2**), in the presence of HOBt and *N*-methyl morpholine in DMF. The methyl ester and trifluoroacetyl protecting groups were removed simultaneously, with 2.0 N NaOH/EtOH/H₂O (1:11:5), and the product was employed in the subsequent coupling reaction without further purification. 2,4-Diamino-6-(hydroxylmethyl)pteridine was bro-

(17) Wiley, R. A.; Rich, D. H. *Med. Res. Rev.* **1993**, *13*, 327−384.
(18) Jencks, W. P. *Proc. Natl. Acad. Sci. U.S.A.* **1981**, *78*, 4046−4050.
(19) Cheetham, J. C.; Smith, D. M.; Aoki, K. H.; Stevenson, J. L.; Hoeffel, T. J.; Syed, R. S.; Egrie, J.; Harvey, T. S. *Nat. Struct. Biol.* **1998**, *5*, 861−866.
(20) Syed, R. S.; Reid, S. W.; Li, C.; Cheetham, J. C.; Aoki, K. H.; Liu, B.; Zhan, H.; Osslund, T. D.; Chirino, A. J.; Zhang, J.; Finer-Moore, J.; Elliott, S.; Sitney, K.; Katz, B. A.; Matthews, D. J.; Wendoloski, J. J.; Egrie, J.; Stroud, R. M. *Nature* **1998**, *395*, 511−516.
(21) Cunningham, B. C.; Ultsch, M.; de Vos, A. M.; Mulkerrin, M. G.; Clauser, K. R.; Wells, J. A. *Science* **1991**, *254*, 821−825.
(22) Chantalat, L.; Jones, N.; Korber, F.; Navaza, J.; Pavlovsky, A. G. *Protein Peptide Lett.* **1995**, *2*, 333.
(23) de Vos, A. M.; Ultsch, M.; Kossiakoff, A. A. *Science* **1992**, *255*, 306−312.
(24) Bolin, J. T.; Filman, D. J.; Matthews, D. A.; Hamlin, R. C.; Kraut, J. *J. Biol. Chem.* **1982**, *257*, 13650−13662.
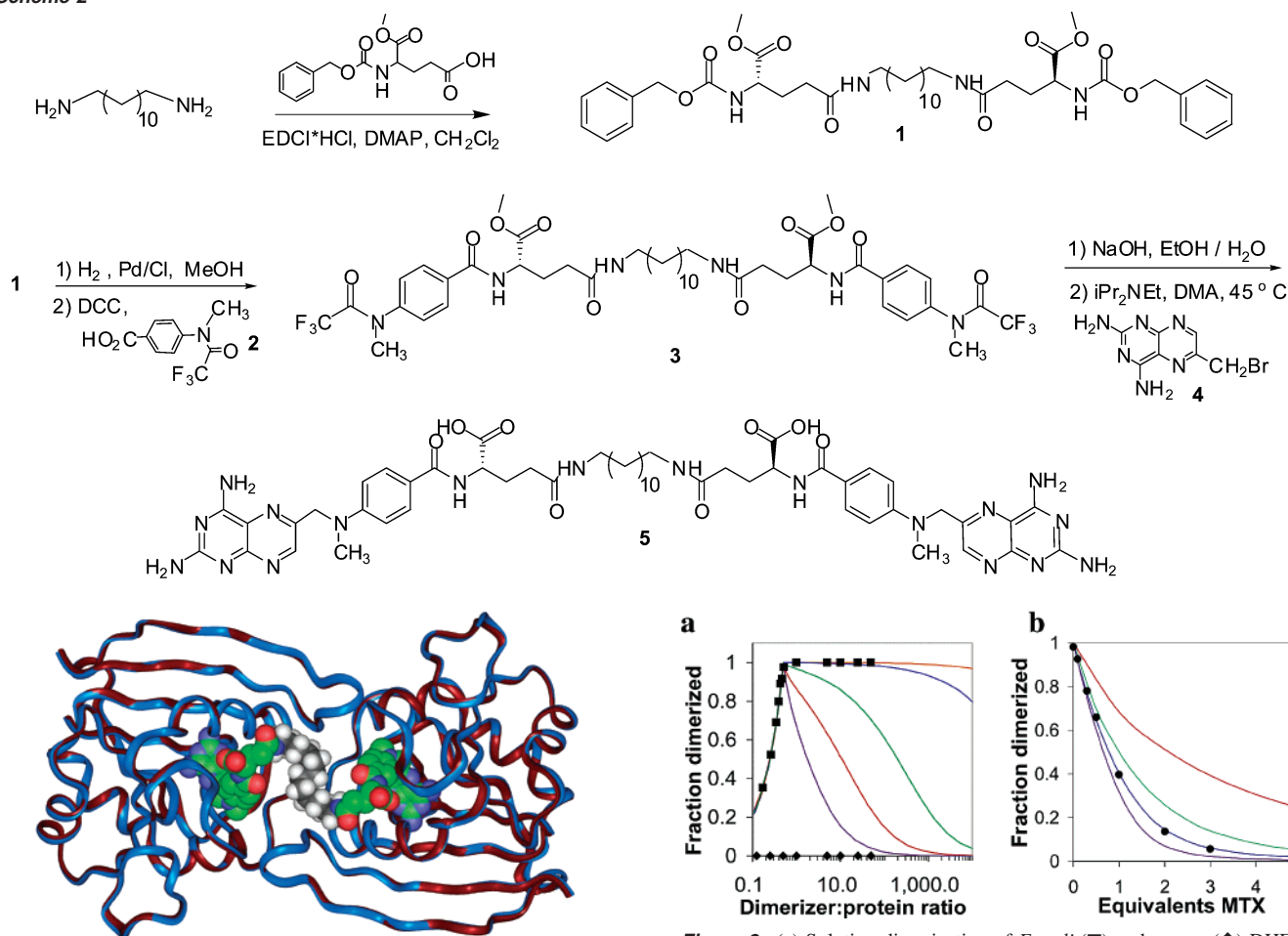(25) Piper, J. R.; Montgomery, J. A.; Sirotnak, F. M.; Chello, P. L. *J. Med. Chem.* **1982**, *25*, 182−187.
(26) Gaggelli, E.; Valensin, G.; Vivi, A. *Magn. Reson. Chem.* **1993**, *31*, 431−434.
(27) Mammen, M.; Shakhnovich, E. I.; Whitesides, G. M. *J. Org. Chem.* **1998**, *63*, 3168−3175.
(28) Kopytek, S. J.; Standaert, R. F.; Dyer, J. C. D.; Hu, J. C. *Chem. Biol.* **2000**, *7*, 313−321.
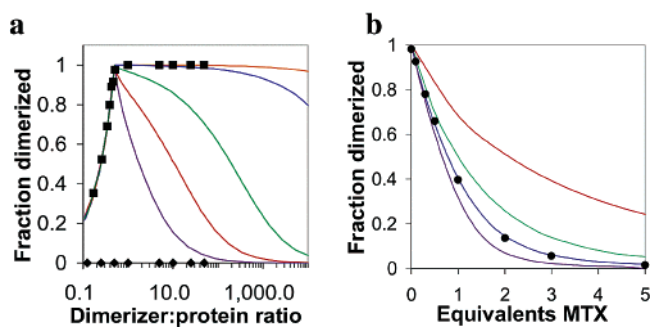
Scheme 2

Figure 1. Crystal structure of DHFR in binary complex with bis-MTX. The figure displays an overlay of the current crystal structure (ribbon in blue, with ligand colored by atom) and the 4DFR structure (ribbon in maroon, with MTX ligands not shown). The linker of bis-MTX is modeled in gray and white.

Figure 2. (a) Solution dimerization of *E. coli* (■) and mouse (♦) DHFR (5 μM) by bis-MTX, as determined by size exclusion chromatography. Fit curves indicate increasing values of K_c [purple = 1, red = 10, green = 200, blue K_c = 175 and K_{eq} = 570; orange K_c = 1200 and K_{eq} = 3900], along with the estimated minimum and maximum fit for the combination of K_c and K_{eq} (vide infra). (b) Competitive displacement of bis-MTX by MTX. Additional fit lines display the effect of varying the K_{eq} to K_c ratio: purple, 10 to 1; blue, 3.25 to 1; green, 1 to 1; red, 0.1 to 1.

minated by addition to dibromotriphenylphosphorane in DMA to yield **4**, which was carried forward in a one-pot reaction. Addition of compound **3** in the presence of diisopropylethylamine afforded bis-MTX (**5**), in an overall yield of approximately 40%. The product was purified by MPLC, yielding fractions that were 90% pure by HPLC. Preparative HPLC was necessary to obtain analytically pure dimerizer, used in all subsequent dimerization experiments.

To explore the molecular basis for the induction of DHFR dimerization, the crystal structure of ecDHFR was determined to 2.4 Å resolution as a binary complex with bis-MTX (Figure 1).

The structure proved isomorphous to the known ecDHFR–MTX complex (4DFR). Unfortunately, the most stable conformation for the bis-MTX linker in the complex was not distinguishable, due to insufficient electron density for this region. However, lateral displacement of the γ-carboxylates, increasing the separation from 9 to 12.8 Å, was observed, which is consistent with modeling studies of their likely orientation in the ternary complex. A representative linker conformation model appears in Figure 1. Contact between the proteins buries 523 Å² of solvent-accessible surface area, consistent with the hypothesis that a dimer of ecDHFR can be obtained with the

bridged ligand and that a closely packed interface could exist between the DHFR molecules in solution.

Solution Dimerization. We also evaluated the ability of bis-MTX to dimerize DHFR in solution. This was carried out with wild-type ecDHFR[29,30] (~18 kDa) and wild-type mouse DHFR (~21 kDa),[31] both of which were purified by methotrexate affinity chromatography and are monomeric in solution. Dimerization of the *E. coli* enzyme was stoichiometric (i.e., 2 equiv of enzyme dimerized per equivalent bis-MTX added), with 96 ± 3% dimerization observed at a dimerizer:protein concentration ratio of 0.5:1. Furthermore, dimerization was strikingly concentration-independent, with complete dimerization observed over a dimerizer:protein ratio range from 0.5:1 to 50:1 (Figure 2a). In contrast, no dimerization of the mouse enzyme was observed at any dimerizer concentration tested (Figure 2a), nor at enzyme concentrations as high as 20 μM (data not shown). Both proteins employed in these experiments were correctly

(29) Baccanari, D. P.; Averett, D.; Briggs, C.; Burchall, J. *Biochemistry* **1977**, *16*, 3566−3572.
(30) Chen, J. T.; Taira, K.; Tu, C. P.; Benkovic, S. J. *Biochemistry* **1987**, *26*, 4093−4100.
(31) Evenson, D. A.; Adams, J.; McIvor, R. S.; Wagner, C. R. *J. Med. Chem.* **1996**, *39*, 1763−1766.
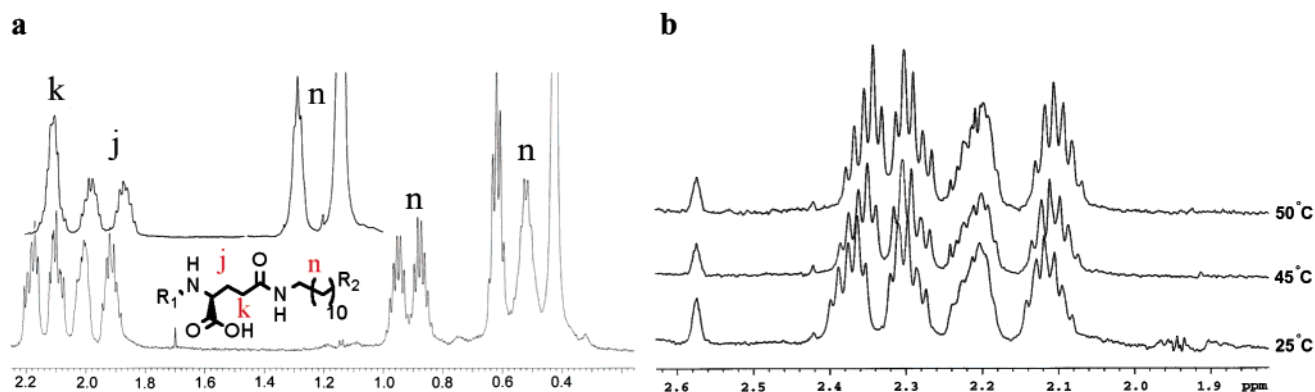
Figure 3. (a) 600 MHz NMR spectra for bis-MTX in DMSO-d_6 (top) and in 80:20 H_2O:DMSO-d_6 (bottom). Inset indicates peak assignments. (b) Overlay of 600 MHz NMR spectra for bis-MTX in 75:25 H_2O:DMSO-d_6 as a function of temperature. Individual spectra are identified at the right of the figure.

folded, catalytically active, and capable of binding bis-MTX, as verified by experimental kinetic and inhibition data.[32] For ecDHFR at pH 7.0 in MTEN buffer (0.1 M NaCl), k_{cat} was determined to be 7.2 s^{-1}; $K_m(H_2F)$, 0.83 ± 0.03 μM; K_i(bis-MTX), 21 ± 7 pM.[33] For mDHFR at pH 7.0, MTEN buffer (0.8M NaCl), k_{cat} was determined to be 50.2 ± 4.0 s^{-1}; $K_m(H_2F)$, 1.91 ± 0.26 μM; K_i(bis-MTX), 48 ± 2 pM.[31]

Because K_{eq} and K_c exert parallel effects on the extension of the dimerization plateau to high ligand concentrations, the solution dimerization data establish only a lower limit for these parameters. The data were fit to a model based on eq 1, using the known K_a value for MTX (1.69×10^9) to closely approximate K_{a1} and K_{a2} (vide supra).[34] Considering cooperativity alone—neglecting the role of ligand conformation—a satisfactory initial fit of the data required a minimum K_c value of 100 000. This result, however, implied 40% dimerization in a 5 μM solution of DHFR and monomeric MTX, where in fact none was observed. We concluded that cooperativity alone could not explain the observed dimerization plateau and proceeded to seek evidence that the hypothesized influence of ligand conformation was in fact at work.

Conformational Analysis of Bis-MTX. We conducted high-field (600 MHz) NMR experiments to probe for conformational restriction in the structure of bis-MTX at room temperature. Spectra collected in 80:20 H_2O:dimethyl sulfoxide-d_6 (DMSO) and in DMSO-d_6 revealed that the γ-protons on the glutamate segments of bis-MTX were diastereotopic in aqueous solution (80:20 H_2O:DMSO), but not in DMSO. Furthermore, whereas the 10 interior methylene protons of the linker were identical (by NMR) in DMSO, three additional signals were resolved in aqueous solution (Figure 3a). In contrast, no diastereotopicity was observed for MTX itself in either solvent system.

To evaluate the nature of this diastereotopicity, we collected NMR spectra of bis-MTX in 75:25 H_2O:DMSO at a series of increasing temperatures (Figure 3b). As the temperature was raised to 50 °C, we observed only partial coalescence of the diastereotopic γ-glutamate protons, suggesting a folded state of reasonable stability.

The apparent conformational restriction of bis-MTX was corroborated by analytical size exclusion chromatography. Whereas elution volumes for globular proteins correlate reason-
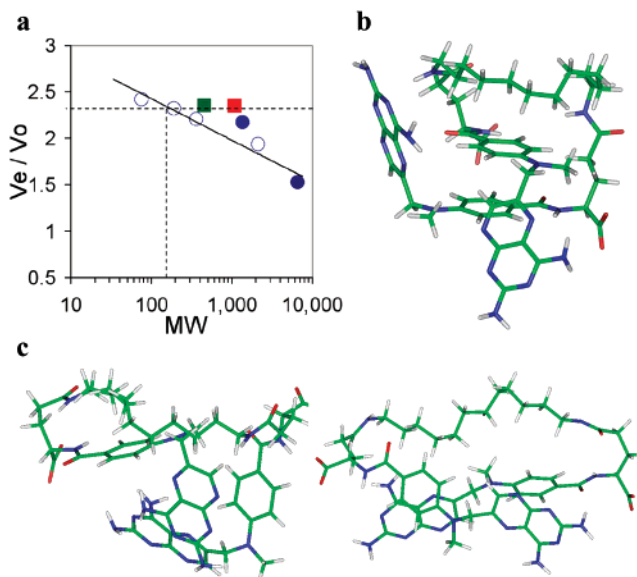
Figure 4. (a) Plot of V_e/V_o (elution volume/elution volume of unretained species) versus molecular weight for MTX (green square) and bis-MTX (red square), as determined by size exclusion chromatography. Circles indicate data for molecular weight standards; filled circles indicate species of known Stokes' radius: vitamin B12 (7.5 Å) and aprotinin (9.83 Å). (b) Compact conformer for bis-MTX upon minimization using cff91 force field in InsightII/Discover. (c) Representative conformers from molecular dynamics simulation of bis-MTX in explicit H_2O.

ably well with calibrated molecular weight, the behavior of compounds on a smaller scale is substantially dependent on molecular shape.[35,36] Bis-MTX (MW = 1073) and MTX (MW = 431) were found to elute at nearly identical rates: a standard calibration curve yielded an apparent molecular weight of 190 $\pm$ 30 Da and estimated Stokes' radius of 7 Å for both compounds (Figure 4a). Given that bis-MTX, fully extended, exceeds 50 Å in length, this experimental estimate for the Stokes' radius suggests an average solution conformation that is highly compact.

Molecular modeling provided a useful tool to investigate the range of feasible sizes for bis-MTX in solution. We began by seeking the smallest possible conformation of bis-MTX. Minimization in vacuo with InsightII/Discover (Accelrys, Inc.) under conditions designed to optimize intramolecular interactions

(32) K_i values were determined by Dixon plot analysis.
(33) Taira, K.; Benkovic, S. J. *J. Med. Chem.* **1988**, *31*, 129−137.
(34) Appleman, J. R.; Howell, E. E.; Kraut, J.; Kuhl, M.; Blakley, R. L. *J. Biol. Chem.* **1988**, *263*, 9187−9198.

(35) Mori, S.; Barth, H. G. In *Size Exclusion Chromatography*; Springer: New York, 1999; pp 17−21.
(36) Himmel, M. E.; Baker, J. O. In *Handbook of Size Exclusion Chromatography*; Wu, C.-s., Ed.; Marcel Dekker: New York, 1995; pp 409−417.

yielded a highly compact, globular minimum size conformer, approximately 15 Å in diameter (Figure 4b). This structure, roughly consistent with the experimental Stokes radius, served as a starting point for molecular dynamics simulations of bis-MTX in explicit solvent. Five simulations were conducted in total, each one a nanosecond or more in length, to thoroughly sample conformational space. Initial conformations included two variants of the minimum-size conformer, two partially folded conformers, and the extended conformation of bis-MTX observed in the ecDHFR−bis-MTX crystal structure. Analysis of the molecular dynamics trajectories revealed a set of well-populated conformational states which were stable on a 500−900 ps time scale and reasonably compatible with the experimental Stokes radii. Representative structures for two of those populations, each with a long-axis dimension of approximately 18 Å, appear in Figure 4c. These compact solution conformations suggest possible structures for a folded form of bis-MTX and illustrate a suite of favorable intramolecular aromatic and hydrophobic interactions which may stabilize that state.

Recent work demonstrating conformational self-association of linked nitrogen heterocycles in aqueous solution lends credence to the notion of stable interactions between the MTX moieties of bis-MTX.[39] It should be noted, however, that careful NMR investigations by Iverson and co-workers have demonstrated that intramolecular interactions in designed aromatic dimers promote an ensemble of folded states rather than a unique folded structure.[40] In this case, K_{eq} would reflect an average stability for the ensemble.

The solution stability of bis-MTX compares favorably to that achieved by various recently reported foldamers—synthetic mimics of biopolymers designed to possess stable secondary structural motifs.[41,42] Phenylene ethylene oligomers, reported by Moore and co-workers, which adopt stable helical conformations in acetonitrile, achieve similar stability for 14-mer repeats ($\Delta G = -4.3$ kcal/mol).[37]

Induced Protein−Protein Interactions. A return to the analysis of solution dimerization reveals that the relative magnitudes of K_{eq} and K_c (a K_{eq}/K_c ratio) can be extracted from a competition binding experiment with MTX (Figure 2b). Adding increasing amounts of monomeric MTX to a solution of preequilibrated protein dimers (bisMTX:ecDHFR = 0.5:1) generates a denaturation curve which can be directly analyzed. Fitting the data to a model based on Scheme 1 yielded a value of 3.25 ± 0.25 for the K_{eq}/K_c ratio.

Incorporating this result into the analysis of the dimerization data allows us to extract minimum values for both parameters: $K_c \geq 175$ ($\Delta G_c \leq -3.1$ kcal/mol), and $K_{eq} \geq 570$ ($\Delta G_{fold} \leq -3.8$ kcal/mol) (Figure 2a).

Given a known K_{eq}/K_c ratio, a method to estimate maximum values for K_c and K_{eq} can also be derived from the dimerization data. As discussed above, large values of K_c imply spontaneous dimerization of the monovalent MTX-ecDHFR complex at high concentrations. Further gel-filtration experiments revealed no detectable dimerization of the MTX-ecDHFR at concentrations as high as 24 μM (data not shown). With a detection error of five percent or less, the absence of observable dimerization at 24 μM implies that K_c is less than 1200. By translation, the maximum value for K_{eq} can be estimated: $K_{eq} \leq 3900$. The free energy range for both dimerization cooperativity and bis-MTX folding can therefore be estimated: $\Delta G_{coop} = -3.1$ to -4.2 kcal/mol; $\Delta G_{fold} = -3.8$ to -4.9 kcal/mol.

Two observations arise from this result: first, the protein surface serves, in essence, *to enhance MTX binding to ecDHFR by at least 175-fold; second, surface differences between ecDHFR and mDHFR create a $\geq 10^7$ fold selectivity for ecDHFR dimerization by bis-MTX.*

Examination of the surface of a mouse DHFR model (data not shown), derived from a human DHFR−MTX crystal structure, PDB accession 1DLS,[44] reveals that the region surrounding the γ-carboxylate tail is both sterically crowded and populated with a preponderance of positively charged residues. These factors are likely to play a major role in impeding mouse DHFR dimerization.

The apparent amplification of bis-MTX affinity by protein surface complementarity echoes a strategy, described by Wandless and co-workers, that employs heterodimerizing bivalent ligands for environment-specific affinity modulation.[43] Recognizing that a given molecular target may be found in varying proteomic environments, they proposed that suitable bivalent ligands might be selectively activated or detoxified by the presence of a second protein. They synthesized bivalent ligands capable of heterodimerizing FKBP12 and the Fyn SH2 domain and demonstrated the capacity of the presenter protein (FKBP12) to reduce ligand affinity for the target protein (Fyn SH2). In the present instance, the ability of ecDHFR to enhance bis-MTX binding demonstrates the feasibility of the complementary case, in which a presenter protein enhances ligand−target affinity.

Often, the free energy of these conformational and binding processes is conceptualized in the easily envisioned form of enthalpy and the integral role of entropy forgotten.[45] While a full treatment of entropic considerations in this dimerization system is beyond the scope of this report, the known entropic penalties of a restricted linker conformation in the protein dimer must be acknowledged. Bis-MTX adopts a folded conformation and dimerizes DHFR cooperatively despite considerable entropic hurdles. Per the method of Whitesides and co-workers,[27] the entropic cost, ΔS_{tor}, of completely restricting torsional movement in the methylene linker is approximately 6 kcal/mol at 298 K. This likely represents an upper limit, as both serpentine movement of the linker in the cooperatively restricted form (as evidenced by the lack of specific electron density in the X-ray crystal structure) and intrinsic flexibility of the folded state function to preserve torsional freedom. Experiments to elucidate the balance of entropy and enthalpy in the molecular components of this system are underway and will be reported in due course.

Conclusions

The implications of our protein dimerization model are several. First, the development of foldamers may profit from

(37) Prince, R. B.; Saven, J. G.; Wolynes, P. G.; Moore, J. S. *J. Am. Chem. Soc.* **1999**, *121*, 3114−3121.
(38) Mammen, M.; Simanek, E. E.; Whitesides, G. M. *J. Am. Chem. Soc.* **1996**, *118*, 12614−12623.
(39) McKay, S. L.; Haptonstall, B.; Gellman, S. H. *J. Am. Chem. Soc.* **2001**, *123*, 1244−1245.
(40) Zych, A. J.; Iverson, B. L. *J. Am. Chem. Soc.* **2000**, *122*, 8898−8909.
(41) Gellman, S. H. *Acc. Chem. Res.* **1998**, *31*, 173−180.
(42) Hill, D. J.; Mio, M. J.; Prince, R. B.; Hughes, T. S.; Moore, J. S. *Chem. Rev.* **2001**, *101*, 3893−4012.

(43) Lewis, W. S.; Cody, V.; Galitsky, N.; Luft, J. R.; Pangborn, W.; Chunduru, S. K.; Spencer, H. T.; Appleman, J. R.; Blakley, R. L. *J. Biol. Chem.* **1995**, *270*, 5057−5064.
(44) Rosen, M. K.; Amos, C. D.; Wandless, T. J. *J. Am. Chem. Soc.* **2000**, *122*, 11979−11982.
(45) Mammen, M.; Choi, S.-K.; Whitesides, G. M. *Angew. Chem., Int. Ed.* **1998**.

the further analysis of the substantial stability generated by these minimal building blocks. Second, optimization of chemical inducers of protein dimerization or other polyvalent ligands must account for the apparent ability of the molecular structure to stabilize conformational states that reduce the accessibility of the ligand to the target binding sites. The frequency of methotrexate-like aromatic or heteroaromatic functionality in drug molecules suggests that a folding propensity may appear in dimeric ligands based on other pharmacophores. If so, this sharpens the design challenge of balancing the conformationally accommodating characteristics of flexibility against the entropic and folding-inhibition benefits of rigidity.

Finally, although the value of K_{eq} for bis-MTX is quite large, a value even 100-fold smaller would still exert a substantial influence on the binding profile of a biological or synthetic dimerizer. This is particularly true when the kinetic aspects of dimerization and signaling are taken into account. A discrete conformational equilibrium introduces a separation between binding thermodynamics and kinetics: while the concentration dependence of ligand binding is governed by the effective K_{a1} (K_{a1}/K_{eq}), the off rate will depend on K_{a1} itself. In the case of cell surface receptors, the duration of binding determines the effective area a monomeric ligand−receptor complex can search for a dimerization partner and therefore the probability of initiating a signal.[46] This phenomenon may be significant in regulating cell-surface receptor dimerization in vivo. Investigations into conformational regulation by biological ligands, the molecular basis for bis-MTX folding, and the implementation of this system in the study of other inducible dimerization processes are ongoing.

Methods

Materials. ^{1}H NMR spectra were obtained using a Varian VAC-300 spectrometer. Reverse-phase HPLC was preformed on a Spectra Physics SP8800 HPLC pump connected to a Kratos Spectroflow 757 detector set at 302 nm using binary gradients formed from solvent A (H_2O + 0.1% v/v TFA) and solvent B (acetonitrile + 0.08% TFA). Analytical HPLC was performed using a Waters Spheris Orb C8 column (4.6 × 250 mm), while preparative HPLC was performed using an Alltech Econosphere C8 column (10 × 250 mm). A two-part linear gradient (min/% B, 0/30, 20/40, 25/30) was used for analytical and preparative HPLC with flow rates of 1.0 and 6.0 mL/min, respectively. Analytical TLC was performed on aluminum-backed silica gel (grade 60) plates obtained from EM Science. Flash chromatography and MPLC were performed with grade 60, 230−400 mesh silica gel from EM Science. Anhydrous DMA and DMF were purchased from Aldrich Chemical Co. and used without further purification. All other chemicals used were purchased from Aldrich or Acros and were used without further purification. All other solvents were reagent grade and used as received.

Synthesis. 1,12-Di-(4-benzyloxycarbonylamino-4-(4S)-methoxycarbonyl-butyrylamino)dodecane (1). Cbz-L-glutamic acid α-methyl ester (1.34 g, 4.52 mmol) and Et₃N (1.9 mL, 9.03 mmol) were added to a stirring solution of 1,12-diaminododecane (0.303 g, 1.51 mmol), 1-ethyl-3-(3-dimethylaminopropyl)carbodiimide hydrochloride (1.34 g, 4.52 mmol), and 4-(dimethylamino)pyridine (0.193 g, 1.58 mmol) in CH_2Cl_2 (20 mL) under an Ar atmosphere. After 18 h the reaction mixture was diluted with CH_2Cl_2 (20 mL) and washed with saturated $NaHCO_3$ (20 mL), 5% KH_2PO_4 (20 mL), H_2O (20 mL), and brine (10 mL). The organic layer was dried (Na_2SO_4) and concentrated under

reduced pressure. Flash chromatography on a silica gel column (3 × 10 cm), eluting with 1% $MeOH/CHCl_3$ (200 mL) and 3% $MeOH/CHCl_3$ (500 mL), gave the desired product (1.02 g, 1.35 mmol, 89.2%) as a flaky colorless solid. TLC R_f = 0.64 $CHCl_3/MeOH$ (9:1). ^{1}H NMR ($CDCl_3$) δ 1.25 (s, 16 H), 1.45 (s, 4 H), 1.95 (m, 2 H), 2.23 (m, 6 H), 3.06 (d, 4 H, J = 7 Hz), 3.73 (s, 6 H), 4.90 (q, 2 H, J = 6, 8 Hz), 5.10 (s, 4 H), 5.80 (d, 2 H), 6.00 (bt, 2 H), 7.34 (m, 10 H).

4-[N-Methyl-N-(trifluoroacetyl)amino]benzoic Acid (2). 2 was synthesized as described by Rosowsky et al.[47] Yield (56.3%). Mp 175−176 °C. TLC R_f = 0.29 Hex/EtOAc (1:3). ^{1}H NMR (MeOH-d_4) δ 3.29 (s, 3 H), 7.45 (d, 2 H, J = 9 Hz), 8.08 (d, 2 H, J = 9 Hz).

1,12-Di-(4-(4S)-methoxycarbonyl-4-[4-(methyl(trifluoroacetyl)amino)benzoylamino]butyrylamino)dodecane (3). Acetyl chloride (0.060 mL, 0.838 mmol) was mixed with MeOH (5 mL), and the resulting methanolic HCl was used to dissolve compound **1** (0.316 g, 0.419 mmol). The solution was flushed with Ar before the addition of 10% Pd/C (0.062 g) catalyst. The mixture was stirred vigorously, and the system was flushed with H_2. The reaction was complete by TLC after 2.5 h, whereupon it was diluted with MeOH (20 mL) and filtered through Celite. The filtrate was stripped of solvent under reduced pressure and dried under high vacuum to yield a greenish white solid (0.229 g, 0.410 mmol, 97.9%). To this material were added DCC (0.338 g, 1.64 mmol) and 4-[N-methyl-N-(trifluoroacetyl)amino]benzoic acid (**2**) (0.355 g, 1.4 mmol), dissolved in dry DMF (5 mL) and 1-hydroxy-benzotriazole hydrate (0.111 g, 0.820 mmol) under an Ar atmosphere at 0 °C. An additional amount of dry DMF (4 mL) and N-methylmorpholine (0.09 mL, 0.820 mL) was added, and after 3 h the reaction was allowed to warm to room temperature. After 20 h, no starting material was visible by TLC using ninhydrin stain. The addition of water resulted in the precipitation of dicyclohexyl urea, which was removed by filtration and washed with cold DMF. The filtrate was evaporated to dryness under reduced pressure, yielding a yellowish white solid (1.03 g). Flash chromatography on a silica gel column (3 × 12 cm), eluting with 4:1:1 Hex/EtOAc/MeOH, 4:4:1 Hex/EtOAc/MeOH, and 1:3:1 Hex/EtOAc/MeOH, yielded the desired product (0.344 g, 0.364 mmol, 88.8%) as a white solid. ^{1}H NMR ($CDCl_3$) δ 1.21 (s, 16 H), 1.44 (s, 4 H), 2.22 (m, 4 H), 2.41 (m, 4 H), 3.21 (m, 4 H), 3.38 (s, 6 H), 3.78 (s, 6 H), (q, 2 H), 7.37 (d, 2H, J = 8 Hz), 8.00 (d, 2 H, J = 8 Hz).

2,4-Diamino-6-(bromomethyl)pteridine (4). Bromine (0.169 mL, 3.30 mmol) was slowly added, over 20 min, to a stirring solution of triphenylphosphine (0.902 g, 3.44 mmol) in cold (0 °C) dry DMA (2.7 mL) under an Ar atmosphere. The reaction mixture was maintained under Ar and allowed to stand for 30 min. In one proportion, 2,4-diamino-6-(hydroxylmethyl)pteridine (0.210 g, 1.09 mmol) was added to the reaction mixture, which was then allowed to warm to room temperature. The reaction was allowed to proceed for 27 h before initiating the subsequent final coupling reaction in the same vessel.

1,12-Di-[4-(4S)-carboxy-4-{4-[(2,4-diaminopteridin-6-ylmethyl)-methyl-amino]-benzoylamino}butyrylamino]dodecane (5) (Bis-MTX). Compound **3** (0.3443 g, 0.364 mmol) was dissolved in a mixture of EtOH (11.1 mL), H_2O (5.5 mL), and 2.0 N NaOH (1.1 mL) and stirred. Once the starting material had disappeared by TLC (3 h), 10% AcOH/H_2O (10 mL) was added and the mixture was acidified to pH 5.5 by addition of 1 N HCl. The acidic solution was extracted with $CHCl_3$ (6 × 30 mL) and EtOAc (2 × 30 mL). The organic fractions were combined, dried over $MgSO_4$, and evaporated under reduced pressure to yield a foamy white solid (0.223 g), used without further purification. The material was taken up in DMA (3 mL) and added to the reaction mixture of compound **4** along with diisopropylethylamine (0.190 mL, 1.09 mmol). Upon addition of base the reaction was heated (45 °C) and maintained under Ar for 25 h. The resulting black mixture was poured into a large volume of 0.33 N NaOH (60 mL) and the

(46) Pearce, K. H., Jr.; Cunningham, B. C.; Fuh, G.; Teeri, T.; Wells, J. A. *Biochemistry* **1999**, *38*, 81−89.

(47) Rosowsky, A.; Freisheim, J. H.; Bader, H.; Forsch, R. A.; Susten, S. S.; Cucchi, C. A.; Frei, E., 3rd. *J. Med. Chem.* **1985**, *28*, 660−667.

insoluble portion removed by filtration. The filtrate was acidified to pH 3.0 by the careful addition of 3.0 N HCl and the resulting solid collected by filtration. Drying of the solid under high vacuum yielded a dark yellow solid (0.286 g). Further purification was obtained by taking 0.106 g of the solid up in $CHCl_3/MeOH/H_2O$ (5:3:0.5) + 1% NH_4OH and injecting it onto a MPLC column, eluting with $CHCl_3/MeOH/H_2O$ (5:3:0.5). MPLC yielded pure (90% by HPLC) and mixed fractions (78% by HPLC) containing the MTX_2-C12 dimerizer. Subsequent pooling and rotoevaporation of the pure and mixed fractions resulted in 42.4 and 23.8 mg, respectively, of orangish brown solid (total reaction yield 46.5%). Bis-MTX (**5**) (1.7 mg) was obtained in analytically pure form by semipreparative HPLC. ^{1}H NMR (DMSO-d_6) δ 1.17 (s, 16 H), 1.31 (s, 4 H), 1.94 (m, 4 H), 2.05 (m, 4 H), 2.95 (q, 4 H, $J = 6$ Hz), 3.18 (s, 6 H), 3.99 (bs, 2 H), 4.75 (s, 6 H), 6.82 (d, 4 H, $J = 9$ Hz), 7.62 (d, 4 H, $J = 9$ Hz), 8.56 (s, 2 H). ESI MS: m/e (relative intensity) 1095.5 (M+ Na, 86), 1073.4 (M^+, 100), 537.3 (41), 308.1 (38). Analytical HPLC t_R = 20.5 min.

Crystallography. The structure crystallized in the space group $P6_1$ with two enzyme complexes in the asymmetric unit of the crystal. Difference electron density maps revealed density for MTX in both enzymes, but no density for the C_{12} bridge of bis-MTX, nor any cofactor density for $NADP^+$. Coordinates from ecDHFR-MTX binary complex (3DRC.pdb) were used as a search model for the rotation and translation searches using the program CNS.[48] The initial rigid body refinement of ecDHFR resulted in $R = 0.255$ with $R_{free} = 0.240$ for all data to 2.4 Å resolution. Further refinement with simulated annealing techniques resulted in $R = 0.202$ and $R_{free} = 0.235$ for all data for the current model of two ecDHFR, one bis-MTX, one Ca^{2+} ion, and 20 water molecules.

Modeling. All simulations were conducted with the cff91 force field in the Discover3 package on InsightII (Accelrys). The minimum size conformer was determined in vacuo as follows: after a random set of 10 initial conformations was generated by high-temperature dynamics, each conformer was subjected to repeated cycles of dynamics (10 ps) and minimization, under conditions which maximized the contribution of Vanderwaals interactions (dielectric constant set to 80). The calculated energy was tracked with each cycle and the process suspended when minimization converged on a stable low-energy compact conformer, Figure 4b.

Molecular dynamics simulations were conducted under periodic boundary conditions, with bis-MTX solvated in a 36−40 Å cubic box. Structures were recorded every picosecond, after an initial 5 ps equilibration period, to generate a trajectory for each simulation. Conformational clustering was evaluated by graphical RMSD analysis (heavy atoms) of all pairs within a given trajectory. The two conformations which appear in Figure 4 represent populations with observed lifetimes of 400−800 ps.

Analytical Gel Filtration. MTX (25 μM) and bis-MTX (12.5 μM) were prepared in P500 buffer with 5% glycerol and chromatographed on a Superdex Peptide HR column (MW range 100−7000 Da, Amersham Pharmacia). Elution volumes (P500 buffer) for a series of molecular weight standards were also measured and used to calculate

the apparent molecular weight of MTX and Bis-MTX by linear regression. Stokes' radii for aprotinin, 9.83 Å (MW = 6500), (data not shown) and vitamin B12, 7.5 Å (MW = 1355),[49] were used to calculate an approximate Stokes' radius of 7 Å for MTX and bis-MTX.

Protein Gel Filtration. ecDHFR and mDHFR (5 μM) were incubated in P500 buffer (0.5 M NaCl, 50 mM potassium phosphate, 1mM EDTA, pH 7.0) with 5% (v/v) glycerol for a minimum of 3 h with varying amounts of bis-MTX in final stoichiometric ratios of dimerizer:protein ranging from 0.1:1 to 50:1. The mixture was then fractionated on a Sephadex G-75 size exclusion column (Amersham Pharmacia), eluting with P500 buffer, and the amount of monomeric and dimeric protein quantitated by absorbance at 280 nm.[28] Dimerization was shown to have reached equilibrium, as incubations conducted for as long as 5 days gave identical results; no significant difference was observed when NADPH (100 μM) was included in the dimerization buffer (data not shown). Microsoft Excel was used to model the dimerization data as a function of free ligand concentration. The expression for free enzyme concentration below is the basic expression from which the concentrations of the remaining species can be derived.

$$[E] = \frac{-(1 + K_{a1}[D_a]) + \sqrt{(1 + K_{a1}[D_a])^2 + 8K_{a1}K_{a2}K_c[D_a]E_t}}{4K_{a1}K_{a2}K_c[D_a]}$$

For competition experiments, preequilibrated (3+ hours) DHFR dimers in GP500 buffer were mixed with increasing concentrations of monomeric MTX. Samples were incubated for 48 h after addition of MTX and then assayed by gel filtration chromatography as described above. Data were fit to the expression below with Mathematica (Wolfram Research), in which manual optimization was used to obtain the best fit, $R^2 = 0.998$. This model used to derive this equation requires that the effective K_2 ($K_{a2}K_c$) be significantly greater than the effective K_1 (K_{a1}/K_{eq}), which is consistent with the values observed here.

$$[E_2D_{active}*] = \frac{K_cK_{a1}K_{a2}\,(0.5 - [E_2D_{active}*])(1 - 2[E_2D_{active}*])^2}{K_{eq}K_{aMTX}{}^2(M_t - E_t + 2[E_2D_{active}*])^2}$$

Supporting Information Available: Spectra of compounds prepared in this study. This material is available free of charge via the Internet at http://pubs.acs.org.

JA026264Y

(48) Brunger, A. T.; Adams, P. D.; Rice, L. M. *Structure* **1997**, *5*, 325−336.

(49) Sober, H. A.; Harte, R. A.; Sober, E. K.; CRC Press: Cleveland, OH, 1968; pp C10−C30.